CATHARE-3: A first computation of a 3-inch break Loss-Of-Coolant Accident using both Cartesian and cylindrical 3D-meshes modeling of a PWR vessel

R. Prea, V. Figerou, A. Mekkas, A. Ruby

CATHARE-3: A FIRST COMPUTATION OF A 3-INCH-BREAK LOSS-OF-COOLANT ACCIDENT USING BOTH CARTESIAN AND CYLINDRICAL 3D-MESHES MODELING OF A PWR VESSEL

R. Prea[1], V. Figerou[2], A. Mekkas[1], A. Ruby[2]
CEA – Commissariat à l'Energie Atomique et aux Energies Alternatives
DEN/DM2S/STMF – Service de Thermohydraulique et de Mécanique des Fluides
[1]Université Paris-Saclay, F-91191, Gif-sur-Yvette, France.
[2]Centre de Grenoble, 17 rue des Martyrs, 38054 Grenoble cedex 9, France
raphael.prea@cea.fr ; vincent.figerou@cea.fr ; anouar.mekkas@cea.fr ; alain.ruby@cea.fr

ABSTRACT

CATHARE-3 is the new version of the French thermal-hydraulic code for safety analysis of nuclear reactors. It is developed in the framework of the NEPTUNE project launched by the CEA, EDF, AREVA-NP and IRSN in 2001. CATHARE-3 V2.0 was delivered by December 2016.

The paper will focus on a particular test-case, showing the new abilities of CATHARE-3. The PWR vessel has been described using seven 3D-modules, with a Cartesian coordinate meshing for the core (with one cell per assembly in a horizontal section) and cylindrical coordinate meshing for the other vessel components (downcomer, upper and lower plena …). Using this modeling, a 2,800s simulation of a 3-inch-break Loss-Of-Coolant Accident (LOCA) in one of the PWR cold legs has been run and compared to results with a CATHARE-2 and CATHARE-3 "classical" modeling for the vessel (with only cylindrical grids).

This computation has been made possible by the development of non-conformal junctions between Cartesian coordinates and cylindrical coordinates. A similar computation is not possible with CATHARE-2 because non-conformal junctions are not available. Many analytical verification test-cases of the non-conformal junctions have also been made, checking the mass-flow and energy-flow conservation at the non-conformal junctions on various configurations. These test-cases, showing that an improvement for momentum equations is needed, are also presented in the paper.

This 3D-vessel modeling also shows the abilities of CATHARE-3 to manage a large number of 3D-cells (about 7000 instead of less than 1000 for a typical CATHARE-2 3D-vessel modeling) thanks to the new numerical methods available in CATHARE-3.

This computation demonstrates the potential of CATHARE-3, which should reach the status of an industrial tool available for safety studies in 2019.

KEYWORDS

CATHARE-3, System codes, 3D-vessel, Non-Conformal junctions, LOCA

1. INTRODUCTION

CATHARE-3 is the new version of the French thermal-hydraulic code for safety analysis of nuclear reactors. Its development has begun in 2006 as part of the NEPTUNE project launched by the CEA, EDF, AREVA-NP and IRSN in 2001 [1]. A first validated version of the code, V2.0, was delivered by December 2016, in the continuity of the reference multi-concept CATHARE-2 [2]. This article first presents the major improvements of CATHARE-3 V2.0, especially the 3D features.

Then, the paper will focus on a particular test-case, showing the new abilities of CATHARE-3: The PWR vessel has been described using seven 3D-modules, with a Cartesian grid for the core (with one cell per assembly in a horizontal section) and cylindrical grids for the other vessel components (downcomer, upper and lower plena …). Using this modeling, a 2,800s simulation of a 3-inch-break Loss-Of-Coolant Accident (LOCA) in one of the PWR cold legs has been run and compared to results with a CATHARE-2 and CATHARE-3 “classical” modeling for the vessel (with only cylindrical coordinate meshing).

With the delivery of CATHARE-3 V2.0, a verification report of the 3D module has also been delivered; the following section shows this verification process.

In the last section before the conclusion, the ongoing and future works will be presented.

2. CATHARE-3 V2.0 FEATURES

2.1. The Validated Version of CATHARE-3

With respect to the current reference code for safety studies, CATHARE-2, the major points of this first validated version of CATHARE-3 are:

- CATHARE-3 is validated on more than one hundred Integral Effect Tests (IET) and Separate Effect Tests (SET) from the CATHARE-2 validation matrix that demonstrate the Non-Regression of CATHARE-3 against CATHARE-2. They confirm that the 6-equation 2-fluid model of CATHARE-3 is reliable, as most of the results superimpose with those of the CATHARE-2. These tests are included in Non-Regression reports delivered with the code.
- CATHARE-3 has optional closure laws for sub-channel analysis (void fraction dispersion, temperature dispersion and diffusion, velocity diffusion), validated on various experiments [3] [4].
- Multi-field models of CATHARE-3 [5] have been improved and their validation extended [6].
- The 3D modelling abilities of CATHARE-3 have been improved (see part 2.2).

Moreover, a dozen of industrial configurations has been run with CATHARE-3 V2.0 including the 3D-vessel calculations presented in part 3.

2.2. From CATHARE-2 to CATHARE-3 for a Modular Modelling of the Vessel

The 3D-module of CATHARE-2 has been validated to model both the whole reactor pressure vessel [7] [8] and some subcomponents of the pressure vessel like the core [9] or the downcomer [10] regions from the small to large break LOCAs. A global overview of the CATHARE-2 3D module is available in [11], presenting its basic set of equation and their discretization. CATHARE-3 has the same basic set of equations as CATHARE-2. One of the main goal of CATHARE-3 is to improve 3D modeling of the vessel using thin and non-conformal structured meshes [12].

2.2.1. General approach for the 3D modelling of the vessel in CATHARE-3

In CATHARE-2, only one cylindrical 3D grid is used for the simulation of the whole pressure vessel (see Fig. 1 – center) and it has been proved to be sufficient for simulating any kind of breaks LOCA transients. However, for a better flexibility of the modeling, for the simulation of some transients with significant transverse flow in the core, for neutronic-coupled simulations, or any other 3D flow investigations, a Cartesian 3D meshing of the core and an adapted meshing of the plena would significantly improve the simulation abilities. In CATHARE-3, it has been decided to couple different kinds of 3D modules (one for each component: core, downcomer, plena...). A typical set of grids is (see Fig. 1 – right):

- Cylindrical 3D grids for all the vessel components except the core,
- Cartesian 3D grids (one cell per assembly in a horizontal section and 40 axial meshes) for the core,

As explained in [13], new optimized resolution methods have been developed in CATHARE-3 to couple 3D modules, and the input data-deck syntax has also been adapted to these new functionalities [11].

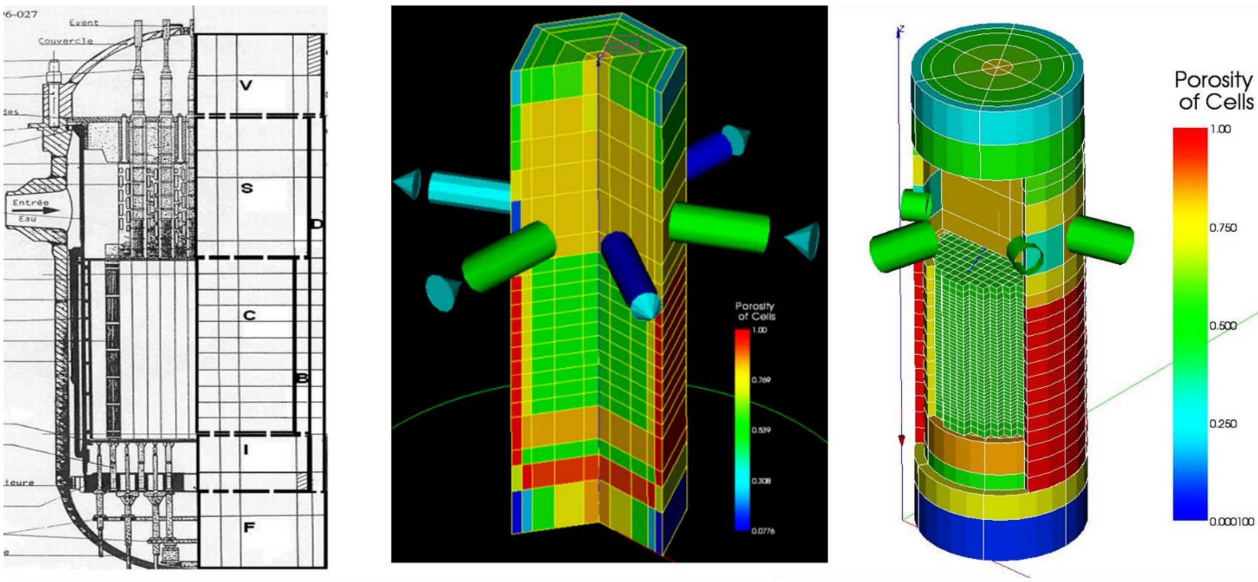

Fig. 1 : Reactor vessel modeled by CATHARE-2 (middle) and CATHARE-3 (right).

2.2.2. The Graphical User Interface of CATHARE: GUITHARE

Creating such type of modeling can be complicated for users, so the CATHARE team has improved the GUITHARE tool (based on the SALOME platform: http://www.salome-platform.org) and the layout data of the 3D modules. GUITHARE stands for Graphical User Interface for caTHARE, it is a common tool for CATHARE-2 and CATHARE-3, including a syntax translator from CATHARE-2 to CATHARE-3 [11] and now adapted to these new 3D abilities.

Most users have a CATHARE-2 modeling of the pressure vessel, in which the 3D vessel is made up of a single 3D module. Using GUITHARE, it is possible to directly translate then split the CATHARE-3 Mono-3D dataset from the HMI, into multiple 3D elements. GUITHARE allows the pre and post-treatment of multiple 3D modules in the same study. Several 3D modules can be grouped together to form a macro-module that is displayed as if it was a single 3D module.

GUITHARE also helps to create Cartesian-cylindrical junctions; the standard way to define the junction between two 3D-modules is to let the user define the geometry and let the code compute the connectivity tables between meshes. This is well adapted when the connection is simple and does not require particular treatments. However, the case of a junction between a Cartesian-meshed core and a cylindrical-meshed plenum is much more complex and we have decided that GUITHARE will calculate the characteristics of the meshing intersection between the two grids and give them to CATHARE-3 for the calculation.

3. FIRST COMPUTATION WITH CATHARE-3 V2.0

The test-case, consisting in a 3-inch break cold leg LOCA with delayed pump-trip, is a reference industrial test-case used as non-regression test for each new CATHARE-2 release.

This test has been analyzed in both CATHARE-2 and a previous version of CATHARE-3: V1.0 [13], in this previous work, the following modeling of the 3D-vessel have been created:

- The reference CATHARE-2 dataset, with a single 3D module for the whole vessel. The results obtained with this modeling are labeled “C2-Mono-3D”. A view of the 3D vessel modeling is available on Fig. 1 (center).
- A first CATHARE-3 dataset has been obtained with the automatic translation of the CATHARE-2 input deck, the results obtained with this dataset are labeled as “C3-Mono-3D”. The comparison between these results and the C2-Mono-3D results will show the non-regression between CATHARE-2 and CATHARE-3.

- A second CATHARE-3 dataset has been obtained using GUITHARE and splitting the C3-Mono-3D dataset into seven 3D modules. The 3D Modules are connected to one another by conforming 3D-3D junctions, the results obtained with this dataset are labeled as “C3-Multi-3D”. Apart from the 3D-3D junctions, the modeling remains unchanged. Comparing results to those obtained with the Mono-3D configuration shows the behavior of the 3D-3D (conforming) junctions.
- A third CATHARE-3 dataset has been obtained with some mesh refinement on the “C3-Multi-3D”. 40 meshes are used instead of 10 along Z in the core region (PERICLES assessment), and 19 meshes instead of 17 along Z in the downcomer (UPTF assessment), and 12 azimuthal meshes instead of 6 in the downcomer, for demonstration purpose. A non-conforming junction connects the downcomer and the vessel bottom, the results obtained with this dataset are labeled as “C3-Multi-3D-NC”. Comparing results to those obtained with the “C3-Multi-3D” configuration shows the behavior of the 3D-3D non-conforming junctions and the refinement effects.

In this paper, a new configuration is presented, replacing the cylindrical core by a Cartesian core (with one cell per assembly in a horizontal section) using Cartesian-cylindrical non-conformal junctions for the core-plena junctions. A view of the 3D vessel modeling is available on Fig. 1 (right).

3.1. Dataset Generation of the Cartesian Core

Thanks to the new syntax abilities of CATHARE-3, the creation of the Cartesian core data deck was simple. Indeed, using new operators and directives (like TABLE, REPEAT …), it is possible to write a compact description of the geometry and the power distribution. CATHARE-3 allows a multiple creation of some objects made into a loop (with the REPEAT directive), for example, it was used for the Fuel Rod creation in the input data deck with a parametric distribution of the radial power.
In the cylindrical core, there is only three radial meshes, so the radial power distribution is limited, as shown on Fig. 2 (left). The Cartesian core allows a thinner distribution of the radial power, as shown on Fig. 2 (middle), a comparison between the two radial profiles is available on Fig. 2 (right). The total power and the axial profile remain identical.
The Cartesian grid can allow a direct use of neutronic calculation results for the radial power profile**.**

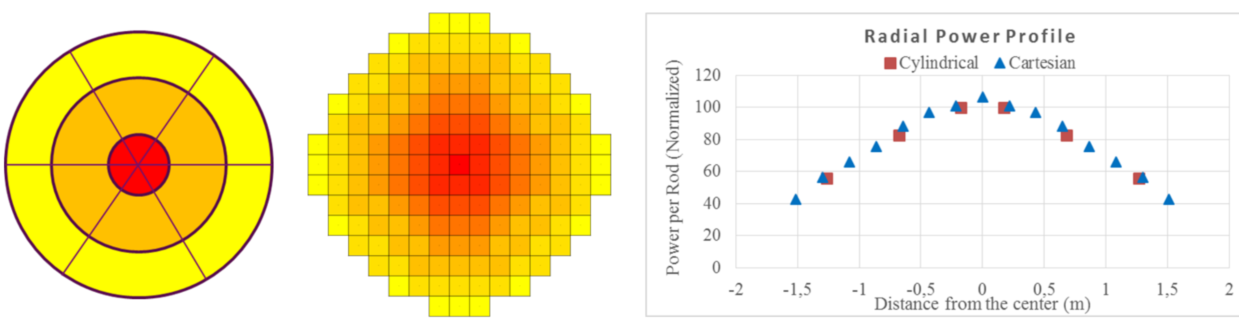

Fig. 2 : Radial power distribution for cylindrical core (left), Cartesian core (middle), and radial power profile (right)

The other part of the data input deck remains identical to those used in the “C3-Multi-3D-NC” configuration. This calculation will provide result with grids adapted to the geometry for both core and downcomer, the main component in which 3D-effect occurs during a LOCA. The results obtained with this dataset are labeled as “C3-Multi-3D-Cart-core”.

3.2. Initial States

The Tab. 1 presents the main parameters of the initial state for the five calculations, deviation between the different calculations remains low. The initial state is obtained by using regulation. No significant dissymmetry between the different loops was observed in any of the calculations, the initial state is very similar for all the calculations.

Tab. 1 : Summary of the initial state

Main parameters of the initial state	C2 Mono-3D	C3 Mono-3D	C3 Multi-3D	C3-Multi-3D-NC	C3-Multi-3D-Cart-core	Maximum deviation (%)
Pressurizer Pressure (bar)	155.7	155.7	155.7	155.7	155.7	0.0
Core ΔT (°C)	35.6	35.6	35.6	35.7	35.7	0.4
HL 1 temperature (°C)	322.2	322.2	322.2	322.3	322.3	0.0
CL 1 temperature (°C)	286.7	286.7	286.6	286.6	286.6	0.0
CL 1 mass flowrate (kg/s)	4,694.0	4,696.6	4,685.1	4,679.1	4,664.1	0.7
SG1 Pressure (bar)	58.4	58.4	58.4	58.4	58.4	0.0
SG2 Pressure (bar)	58.4	58.4	58.4	58.4	58.4	0.0
SG3 Pressure (bar)	58.3	58.3	58.3	58.3	58.3	0.0
SG1 mass flowrate (kg/s)	513.6	513.6	512.8	512.7	517.7	1.0
SG2 mass flowrate (kg/s)	513.6	513.7	512.8	512.7	509.0	0.9
SG3 mass flowrate (kg/s)	517.9	517.9	516.6	516.7	515.7	0.4

3.3. Chronology of the Transients

The Tab. 2 presents the happening time of the main events during the transient, for all the calculations, the break opens at time = 0s and the primary pump coast-down appends at 1,200s for all the calculation (time written in the input deck). The other events occur on signal linked to local values of physical parameters. For short-term events (100s after the break opening), there is a delay of about 10s between the CATHARE-2 calculation and the CATHARE-3 calculations. The reason of this deviation has not been found yet, but it does not have a significant impact on the transient evolution, as shown in the next part. Long-term events are similar between the different calculations.

Tab. 2 : Summary of the transient

Main events during the transient	C2 Mono-3D	C3 mono-3D	C3 multi-3D	C3-Multi-3D-NC	C3-Multi-3D-Cart-core	Maximum deviation (s)
SCRAM signal (s)	18.0	8.6	7.9	7.9	8.8	10.1
Turbine isolation (s)	18.3	8.9	8.2	8.2	9.2	10.1
MFW stopped (s)	23.0	13.6	12.9	12.9	13.9	10.1
ECCS signal (s)	57.2	46.3	45.6	45.7	46.5	11.6
AFW actuated (s)	87.2	76.3	75.6	75.7	76.5	11.6
SG atmospheric dump opening (s)	1,218.0	1,208.6	1,207.9	1,207.9	1,208.9	10.1
PRZ ORV opening (s)	1,218.0	1,242.8	1,221.1	1,207.9	1,208.9	34.8
Accumulators on (s)	1,381.1	1,389.3	1,375.9	1,378.3	1,377.9	13.4

3.4. Evolutions of Main Parameters During the Transient

The evolution of the main parameters can be seen in Fig. 9 in the appendix.

The transient takes place identically over all the different modeling, as shown by the evolution of the global parameters: the primary pressure (Fig. 9 – a) and the liquid break flow (Fig. 9 – b). As the break is small (3 inch), the transient is slow and the core remains wetted even after the primary pumps coast-down (1,200s). From this point, a fall down of the primary pressure is observed and then the accumulator discharge happens. The flow rate of the accumulators is very sensitive to the primary pressure and varies from one calculation to another (Fig. 9 – g – with a zoom on time axis), which explains the differences observed on the liquid mass in the vessel from 1,500s (Fig. 9 – c). Because of the core's drying occurs late, the rod temperature rise relatively slowly (Fig. 9 – h) (compared to a LB-LOCA), thanks to a low power decay. The core reflooding occurs just after the accumulator discharge and it is therefore fast (it lasts about 30s), and there is no steady stabilized swell level in the core during the reflooding phase. Then, the water level in the vessel stabilizes in the upper plenum just below the junctions with the hot leg. The core restart again to boil without being uncover (Fig. 9 – e).

It is important to emphasize that the evolution of external temperature cladding temperature is very similar between the different calculations (Fig. 9 – h).

The following points were noticed: The evolution of the local void fraction in the downcomer (Fig. 9 – f) shows the local effects of azimuthal refinement ("C3-Multi-3D-NC" and "C3-Multi-3D-Cart-core" results are different from the other calculations). In the same way, in the stabilization phase at the end of the transient (Time > 2100s), a lower void fraction is observed at the bottom of the core (Fig. 9 – e) when the core is thinly axially meshed (PERICLES assessment). But the evolutions of the steam mass in the vessel remains similar between all the calculations (Fig. 9 – d), which shows that these local differences due to the refinement, only have a limited effect on the value of the global variables.

3.5. Analysis of the 3D-Core Phenomena

Thanks to the use of a Cartesian grid for the core, the 3D phenomena taking place in it during the transient can be analyzed finely, improving their understanding.

Fig. 10 in the appendix shows the gas velocity field, gas temperature field and void fraction profile during the reflooding of the core. One can notice that the swell level in the whole width is quite homogeneous (void fraction profile) and vapor velocity are mainly vertical, with a weak but existing chimney effect (aspiration towards the center).Then, the radial gas temperature profile is similar to the radial power profile.

The Fig. 11 shows the liquid velocity field and the void fraction field immediately after the core reflooding (then the level of water in the vessel is in the lower part of the upper plenum), one can notice that the core is still boiling in the top part and the void fraction distribution is radially homogeneous thanks to the existence of a well-established liquid recirculation loop.

It should be noticed that the loops of recirculation in the liquid phase are also observed during the reflooding, but these loops are not well established because of the fast transitory aspect of the reflooding.

An analytic analysis of the chimney effect can be found in [14], showing that chimney effect is expected in LOCA situation. A general overview of the 3D-core thermalhydraulics phenomena occurring during PWR LOCA is available in [15].

These phenomena can be compared to experimental observations.

3.5.1. Comparison with the BOIL-UP tests of the PERICLES-2D [9]

The PERICLES 2D experiment has been carried out to investigate multidimensional effects that can occur in a PWR core where the heating power is not radially uniform in both core, uncover and reflooding cases. The experiment consists in a vertical rectangular channel containing three different rod assemblies, the dimensions (in mm) of the assemblies are indicated in Fig. 3 (left). In the BOIL-UP tests, some subcooled water enters into the assemblies from the bottom of the system. The rods are electrically heated and some vaporization occurs along the channel. The flow is successively a single-phase liquid then two-phase mixture and finally single-phase vapor flow. The transition between the two-phase zone and the dry zone (single-phase vapor) occurs at the elevation of the swell level ZG (see Fig. 3 - right). The liquid flow rate at the entrance is regulated in order to have a given stationary position of the swell level.

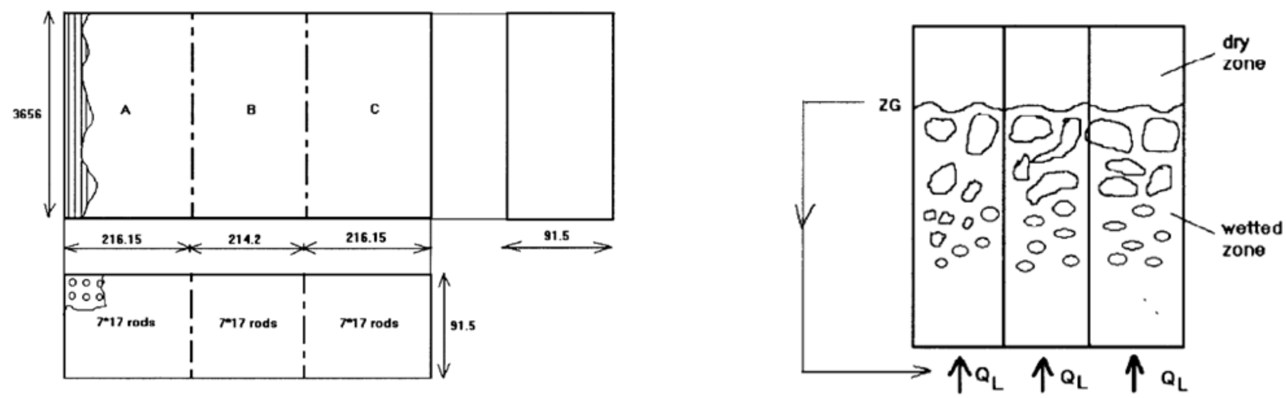

Fig. 3 : The PERICLES 2D experiment (left) and BOIL-UP tests (right)

On the BOIL-UP tests, C. Morel and D. Bestion say that [9]: "*The observed experimental tendencies are the following:*

- *The axial position of the swell level ZG is quite the same for the three assemblies, even if the radial peaking factor, is not equal to 1.*
- *The void fraction profiles in the three assemblies are close to each other, showing the existence of cross-flows in the wetted zone. The wetted zone is thus characterized by a perfect or quasi-perfect radial mixing.*
- *The wall to vapor heat transfer in the dry zone is close to the one obtained by assuming a perfect radial mixing in the wetted zone, a uniform steam flux at the swell level and no radial mixing in the dry zone.*"

These phenomena are also observed in the 3D-core scale calculation.

4. VERIFICATION OF THE 3D MODULE

These test-cases are included in the Non-Regression report with the CATHARE-3 V2.0 delivery at the end of 2016 to the French partners of the CATHARE code, the full-length report contains 88 test-cases [16]. The aim of these test-cases is to show a global and detailed overview of the 3D module of the CATHARE-3 Code. These tests are included in the CATHARE's non-regression data-base and are run daily. The report is automatically generated each day, showing the impact of every new development.

4.1. General Approach

The long-term objective is to reach a total analytical verification of the CATHARE-3 3D vessel modeling previously presented. To complete this goal, the following points are addressed by these test-cases:

1. There are known issues for the 3D module of CATHARE, these are shown and synthesized.
2. Non-Regression between CATHARE-3 and CATHARE-2 is shown using various simple configurations.
3. The 3D-3D junctions are not available in CATHARE-2, therefore some test-cases show their behavior only on CATHARE-3.
4. The 3D-3D non-conformal junctions are not available in CATHARE-2, therefore some test-cases show their behavior only on CATHARE-3.
5. For most of the test-cases, an analytical solution exists, it is compared to the CATHARE results.
6. Show new features of CATHARE-3.

Moreover, in the future, these test-cases will be used to show improvements and evolutions of CATHARE-3's 3D Module.

Most of the test-cases follow the same methodology. The same configuration is declined in 3 different tests:

- From a CATHARE-2 input deck, a pure non-regression test is run to show the non-regression between CATHARE-2 and CATHARE-3 (Mono-3D configuration).

- From the previous configuration, the CATHARE-3 input deck is modified and the 3D module is split into 2 (or more) 3D modules with a conformal junction. Apart from the 3D junctions, the input deck (boundary conditions, imposed power…) remains unchanged. The results are compared to those obtained with the Mono-3D configuration to show the behavior of the 3D-3D conformal junctions.
- From the previous configuration, one 3D module is refined and a non-conformal junction thus links the two 3D. The rest of the input deck remains identical. The results are compared to those obtained with the conformal configuration to show the behavior of the 3D-3D non-conformal junctions. Some test-cases show refinement effects.

There are two kinds of test-cases: the “analytical elementary tests” and the “analytical integral tests”.

4.1.1. The “analytical elementary tests”

Those tests perform an analytical verification of a particular phenomenon, or configuration occurring in a 3D vessel. The Fig. 4 shows a vessel scheme on which some of the configurations tested are represented. These test-cases can be classified into 5 groups:

- Momentum-equation-with-closed-faces test-cases illustrate the behavior of the momentum equation integration in various configurations with constant porosity,
- Momentum-equation-with-porosity test-cases show the behavior of the momentum equation integration with non-constant porosity,
- 3D - 1D test-cases investigate the behavior of 3D - 1D junctions,
- Momentum-equation-with-gravity-effects test-cases address the behavior of non-conformal junctions when there are gravity effects on the junction,
- Cartesian-cylindrical-Non-Conformal-junction test-cases show the behavior of these junctions.

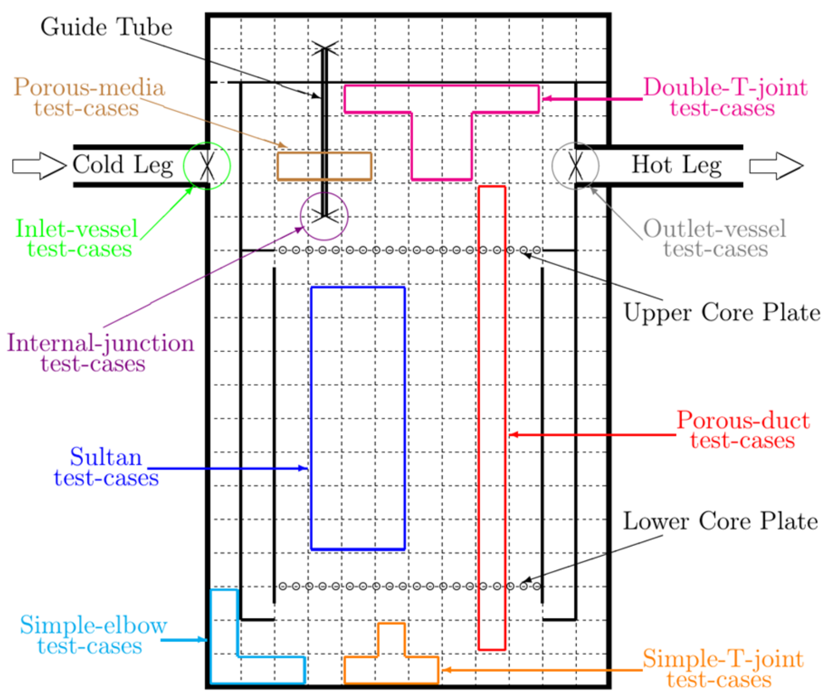

Fig. 4 : Vessel scheme with “analytical elementary” tested configurations

4.1.2. The “analytical integral tests”

Those tests perform a global verification of a simplified 3D vessel. This 3D vessel is representative of a 4-loops PWR vessel (no power source or loss and no head loss are present). A 7 mesh configuration based on a 5x8x8 (R×θ×Z) cylindrical meshing and 5 scenarios for boundary condition evolution are tested. The verification process of these test-cases focus on the existence of a swirling motion within the vessel (when not expected) and on the inlet/outlet symmetry check. The Fig. 5 presents the basis 5x8x8 meshing (left and center) and a tested non-conformal meshing (right); the Tab. 3 presents one of the tested scenarios.

Tab. 3 : Boundary conditions used for the velocity asymmetry scenario

Time **(s)**	**0**	**30**	**60**	**90**	**120**	**150**	**180**	**210**	**240**	**270**
$Q_{\|inlet1}$ **(kg/s)**	3,148	3,148	6,285	6,285	6,285	6,285	6,285	6,285	3,148	3,148
$Q_{\|inlet2,3,4}$ **(kg/s)**	3,148	3,148	3,148	3,148	6,285	6,285	3,148	3,148	3,148	3,148
$T_{liq\|inlet}$ **(°C)**	40	40	40	40	40	40	40	40	40	40
$\alpha_{\|inlet}$	$1.0e^{-5}$	$1.0e^{-5}$	$1.0e^{-5}$	$1.0e^{-5}$	$1.0e^{-5}$	$1.0e^{-5}$	$1.0e^{-5}$	$1.0e^{-5}$	$1.0e^{-5}$	$1.0e^{-5}$
$P_{\|outlet}$ **(bar)**	10	10	10	10	10	10	10	10	10	10

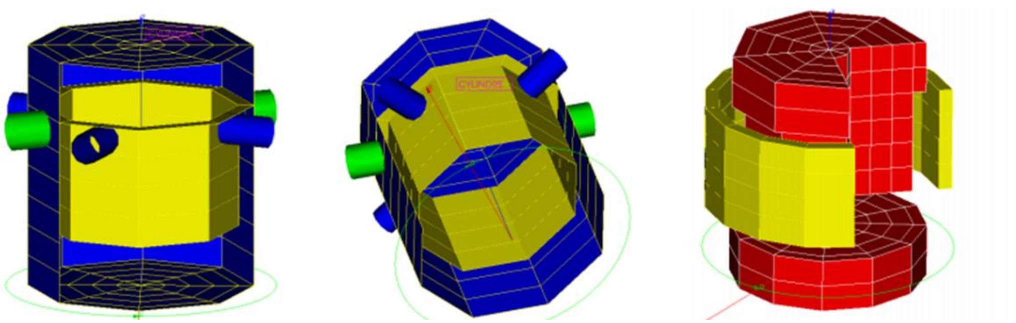

Fig. 5 : 3D vessel views of "analytical integral" tested configurations

4.2. Detailed Example: Porous-Medium Test-Cases

These test-cases model a liquid flow through a porous medium, it is a 2D single-phase flow with any gravity effect. The hydraulic diameter is set very high (D_h = 10^{12} m) to cancel any regular head loss effect. The model does not include any singular head loss either. The Mono-3D configuration consists in a 16x8x1 mesh, where the porosity is set to $\varphi = 1$ (white cells in the Fig. 6) except in the 4x4x1 block located in the middle of the geometry where it has been reduced to $\varphi = 0.5$ (blue cells in the Fig. 6). The porosity distribution is shown in Fig. 6. The Multi-3D configuration inherits from the Mono-3D configuration, but has been split into two 3D elements and contains a conformal junction. The aim of the Multi-3D configuration is to ensure that this junction does not alter the physical results.

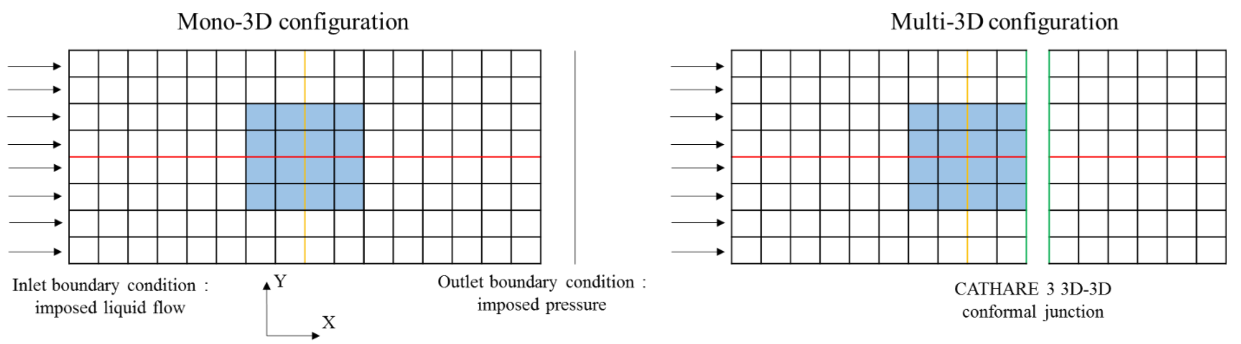

Fig. 6 : Porous media test-cases scheme

An analytical verification has been made on these test-cases:

- The flow should behave symmetrically with respect to the mid YZ plan (red line in the scheme) because of the geometry.
- As well upstream and downstream X-Mass Flow profiles should be identical provided their distance to the center is equal (yellow line in the scheme), while upstream and downstream Y-Mass Flow profiles

should be perfect opposites. It happens because the distances between the obstacle and both upstream and downstream boundary conditions are identical.

There is a good behavior of the Mono-3D computation. But, for the multi-3D computation, the results output some serious deviations in the velocity distribution. The deviations are due to the Cross-momentum terms which have been neglected, so the transverse inertia is lost.

4.3. Detailed Example: Simple Elbow Test-Case

This test models a liquid flow through a simple elbow-shaped duct modeled with a 3D-module. It is a 2D single-phase flow with any gravity effect. The hydraulic diameter is set very high (D_h = 10^{12} m) to cancel any regular head loss effect. There is neither power loss nor source and all cell are identical cube. The Fig. 7 presents a scheme of this test-case.

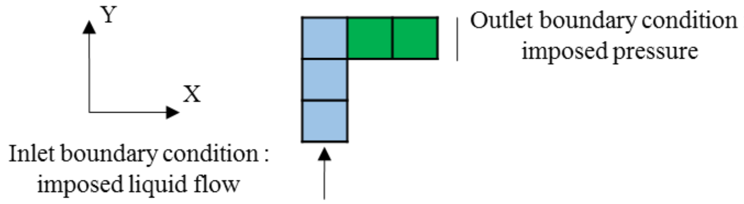

Fig. 7 : Simple elbow test-case scheme

It is worthy of note that no head loss was expected in this test-case. But CATHARE does not pass this test from a verification point of view: a numerical head loss is computed, with head loss coefficient amounts to 1.0. The pressure in the green cells (according to the Fig. 7) is equal to the outlet one; the pressure of the blue cells is given by the formula (1) with V the velocity and ρ the density.

$$P_{in} = P_{out} + \frac{\rho * V^2}{2} \tag{1}$$

5. FUTURE WORKS

This part presents planned works for the next years in the aim to improve 3D behavior and 3D abilities.

5.1. Solving the 3D Issues

There are issues on the momentum balance equations of CATHARE and we plan to solve them.

5.1.1. Momentum balance at 3D-3D junctions

Cross-momentum terms at the junction have been neglected so far. Hence the transverse inertia is lost at each 3D-3D junction. This does not have a significant impact on the system calculation presented in part 3 (comparison between “C3-Mono-3D” and “C3-Multi-3D” calculations) but we plan to resolve this issue and adding an explicit cross term should, at least, be tried.

5.1.2. Elbow numerical head loss

The problem presented in part 4.3 happens in the presence of closed faces and “elbows”, the standard upwind discretization scheme of the convection term of the momentum used in the 3D module of CATHARE does not allow to respect the Bernoulli equation and therefore induces a numerical head loss. These numerical head losses can be suppressed by replacing, locally on the open faces of the elbow, the upwind discretization of the convection term by a centered discretization. This new discretization will be tested on various configurations included in the 3D verification report.

5.2. Spherical Grids

The development of spherical grids for the top and the bottom of the vessel is on-going. The final step will be to have a grid adapted to each component of the vessel and the full description of the reactor vessel described in [12]. No additional work will be necessary to couple a spherical grid with the other components of the vessel. Indeed, in a plane 2D-cut, spherical and cylindrical meshes are identical. Cylindrical-spherical junctions will be treated as cylindrical-cylindrical junctions, already operational in CATHARE-3.

5.3. Validation of CATHARE-3 Using the Non-Conformal Junctions

One of the main points of the V&V process is to have a validation of CATHARE in agreement with the target modeling for industrial applications. This is why the validation will be extended, and the future validation of CATHARE-3 will use multi-3D and non-conformal junctions.
For example, both CATHARE-2 and CATHARE-3 are validated on the UPTF10c experiment [11] which investigates the core upper plate CCFL (Counter-Current Flow Limitation) occurring when steam flows upward from the core and water flows downward, coming from the hot legs. The currently validated modeling uses only one cylindrical grid (Fig. 8 – left). Using CATHARE-3, a possible future validation modeling may use a Cartesian grid for the top part of the core and a cylindrical grid for the upper plenum (Fig. 8 – right).

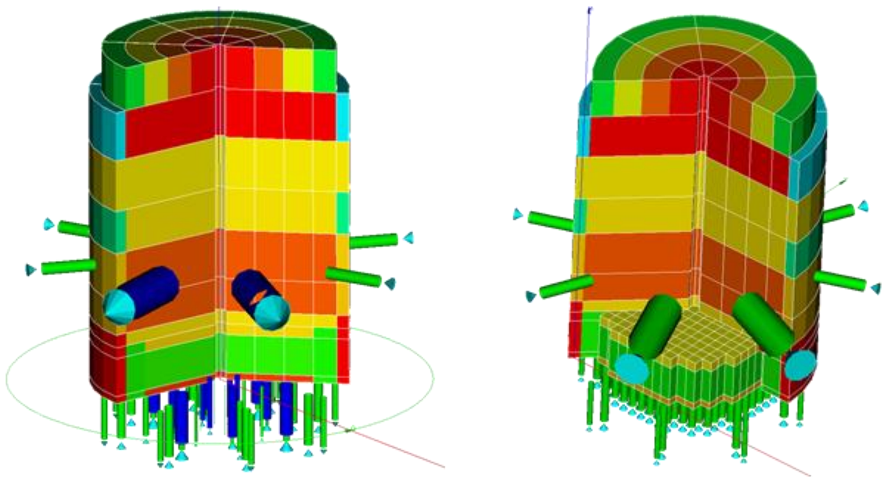

Fig. 8 : UPTF10c modellings with the current meshing (left) and a possible future meshing (right)

The use of a multi-3D modelling of the vessel will also be extended to some IET, like LSTF/ROSA-2 [8].

6. CONCLUSIONS

This 3-inch-break simulation shows an assessment of CATHARE-3 and it demonstrates the 3D abilities of this validated version, it confirms the good behavior of CATHARE-3 for LOCA transients modeling. The use of a Cartesian grid for the core allows comparisons with the experimental observations, and, by analyzing the 3D flows in the core, it improves the 3D-core phenomenon comprehension during LOCA transients.
Moreover, as a non-regression test against CATHARE-2, the 3-inch-break LOCA using a single 3D module was successfully computed by CATHARE-3. And all the presented CATHARE-3 3D vessel modeling are reliable, as shown by comparing the results one to another.
As it has been shown during the 3D module verification process, additional work is necessary in order to use such modeling for safety calculations. This work is planned for the next years. This computation demonstrates the potential of CATHARE-3, which should reach the status of an industrial tool available for safety studies in 2019.
The work presented in this article upholds LOCA safety studies, currently carried out with CATHARE-2, and using a cylindrical modeling of the core.

7. ACKNOWLEDGMENTS

CATHARE-3 is developed in the framework of the NEPTUNE project, financially supported by CEA, EDF, IRSN and AREVA-NP.
The authors want to thanks Yann Di Pasquale and Roberto Freitas from IRSN for their prospective work concerning the validation of CATHARE-3 on UPTF10c experiment using non-conformal junctions.

8. REFERENCES

[1] A. Guelfi, D. Bestion, M. Boucker, P. Boudier, P. Fillion, M. Grandotto, J.M. Herard, E. Hervieu, P. Peturaud, “NEPTUNE A New Software Platform for advanced Reactor Thermalhydraulics”, *Nuclear Science and Engineering,* **156**, pp.282-324, 2007.

[2] O. Antoni, G. Geffraye, D. Kadri, G. Lavialle, B. Rameau, A. Ruby, “CATHARE 2 V2.5_2: a single version for multi-applications”, *Proceedings of 13th International Topical Meeting on Nuclear Reactor Thermal hydraulics (NURETH-13)*, Kanazawa City, Japan, Sep. 27-Oct. 2, 2009.

[3] M. Chandesris, M. Mazoyer, G. Serre and M. Valette, “Rod bundle thermalhydraulics mixing phenomena: 3D analysis with CATHARE 3 of various experiments”, *Proceedings of 15th International Topical Meeting on Nuclear Reactor Thermal hydraulics (NURETH-15)*, Pisa, Italy, May 12-17, 2013.

[4] M. Valette, “Analysis of Subchannel and Rod Bundle PSBT Experiments with CATHARE 3”, *Science and Technology of Nuclear Installations*, Article ID 123426, 2012.

[5] M. Valette, J. Pouvreau, D. Bestion, P. Emonot, “Revisiting Large Break LOCA with the CATHARE-3 Three-Field Model”, *Proceedings of 13th International Topical Meeting on Nuclear Reactor Thermal hydraulics (NURETH-13)*, Kanazawa City, Japan, Sep. 27-Oct. 2, 2009.

[6] M. Spirzewski, P. Fillion and M. Valette, “Prediction of annular flows in vertical pipes with new correlations for the CATHARE-3 three-field model”, *Proceedings of 17th International Topical Meeting on Nuclear Reactor Thermal hydraulics (NURETH-17)*, Xi’an, China, Sep. , 2017.

[7] I. Dor, C. Morel, P. Bazin and P. Boudier, “Assessment of the CATHARE 3D module for LBLOCA simulation”, *Proceedings of 11th International Topical Meeting on Nuclear Reactor Thermal hydraulics (NURETH-11)*, Avignon, France, October 2-6, 2005.

[8] P. Mazgaj, J.-L. Vacher, S. Carnevali, “Comparison of CATHARE results with the experimental results of cold leg IB-LOCA obtained during ROSA-2/LSTF Test 7”, *Proceedings of 2015 International Congress on Advances in Nuclear Power Plants (ICAPP '15),* Nice, France, May 03 - 06, 2015.

[9] C. Morel and D. Bestion, “Validation of the CATHARE code against PERICLES 2D BOIL-UP Tests”, *Proceedings of 9th International Topical Meeting on Nuclear Reactor Thermal hydraulics (NURETH-9)*, San Francisco, California, USA, October 3-8, 1999.

[10] J. Dufrêche and I. Dor, “Assessment of the CATHARE 3D module with UPTF downcomer refill tests” *Proceedings of 40th European Two-Phase Flow Group Meeting,* Norway, 2003.

[11] I. Dor, M. Chandesris, P. Germain and A. Ruby, “CATHARE 3D Module from CATHARE-2 V2.5_3 to CATHARE-3 V1.0”, *Proceedings of 15th International Topical Meeting on Nuclear Reactor Thermal hydraulics (NURETH-15)*, Pisa, Italy, May 12-17, 2013.

[12] P. Emonot, A. Souyri, J.L. Gandrille, F. Barré, “CATHARE-3: A new system code for thermal-hydraulics in the context of the NEPTUNE project”, *Proceedings of 13th International Topical Meeting on Nuclear Reactor Thermal hydraulics (NURETH-13)*, Kanazawa City, Japan, Sep. 27-Oct. 2, 2009.

[13] A. Ruby, P. Emonot, V. Figerou, D. Baloge, A. Fèvre, B. Velly, G. Vigé, “CATHARE-3: First computations of a 3-inch break Loss-Of-Coolant Accident using a modular multi-3D modeling of a PWR vessel”, *Proceedings of 15th International Topical Meeting on Nuclear Reactor Thermal hydraulics (NURETH-15)*, Pisa, Italy, May 12-17, 2013.

[14] D. Bestion, L. Matteo, “Scaling considerations about LWR core thermalhydraulics” *Proceedings of 16th International Topical Meeting on Nuclear Reactor Thermal hydraulics (NURETH-16)*, Chicago, IL, Aug. 30-Sep. 4, 2015.

[15] D. Bestion, M. Valette, P. Fillion, P. Gaillard, “3D-core thermalhydraulics phenomena in PWR SB-LOCAS and IB-LOCAS”, *Proceedings of 17th International Topical Meeting on Nuclear Reactor Thermal hydraulics (NURETH-17)*, Xi’an, China, Sep. , 2017.

[16] R. Prea and F. Guillou, “CATHARE-3 V2.0: Verification of the 3D Module”, *NEPTUNE project report*, CEA, 2016.

APPENDIX

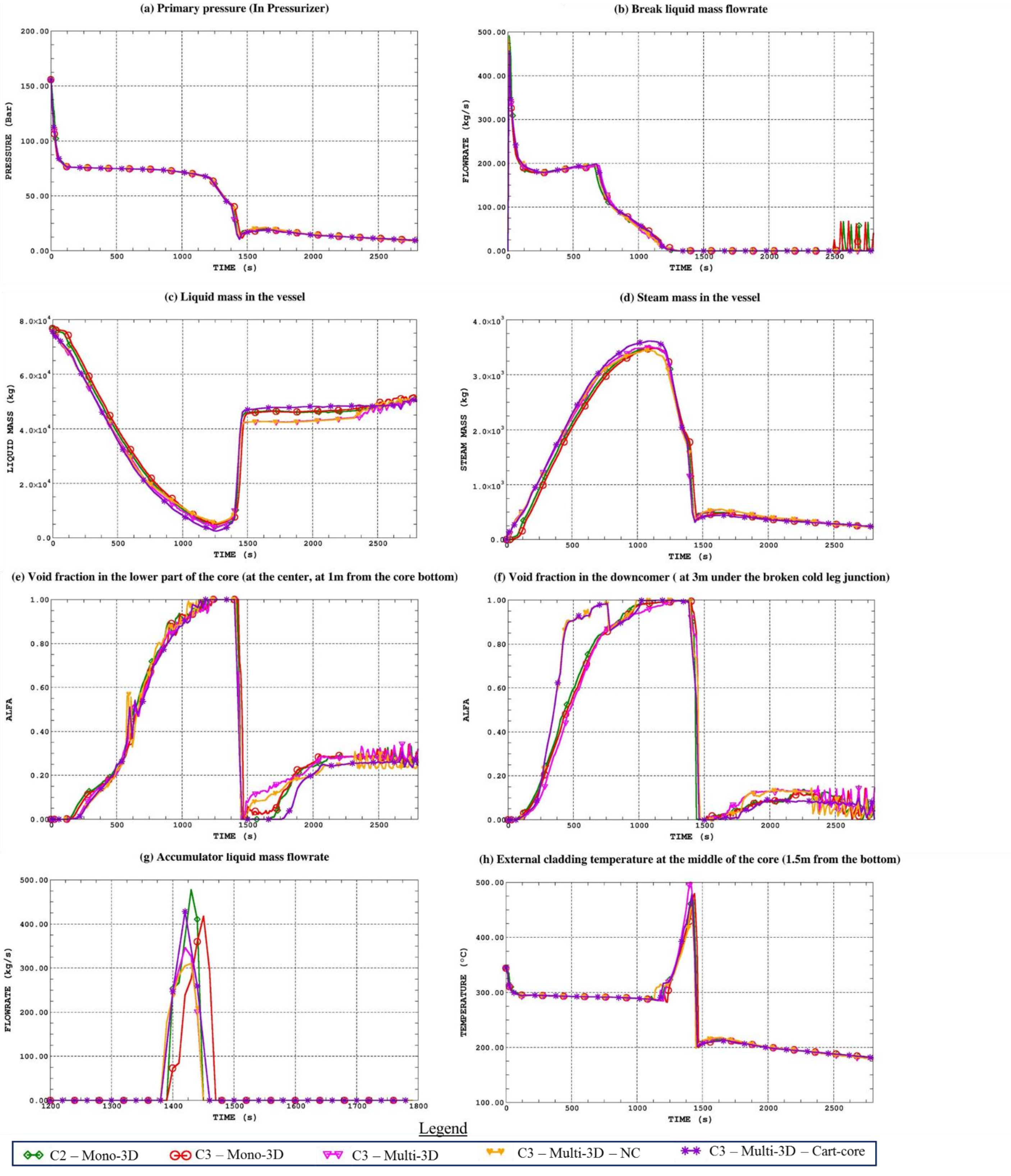

Fig. 9 : Evolution of the main parameters

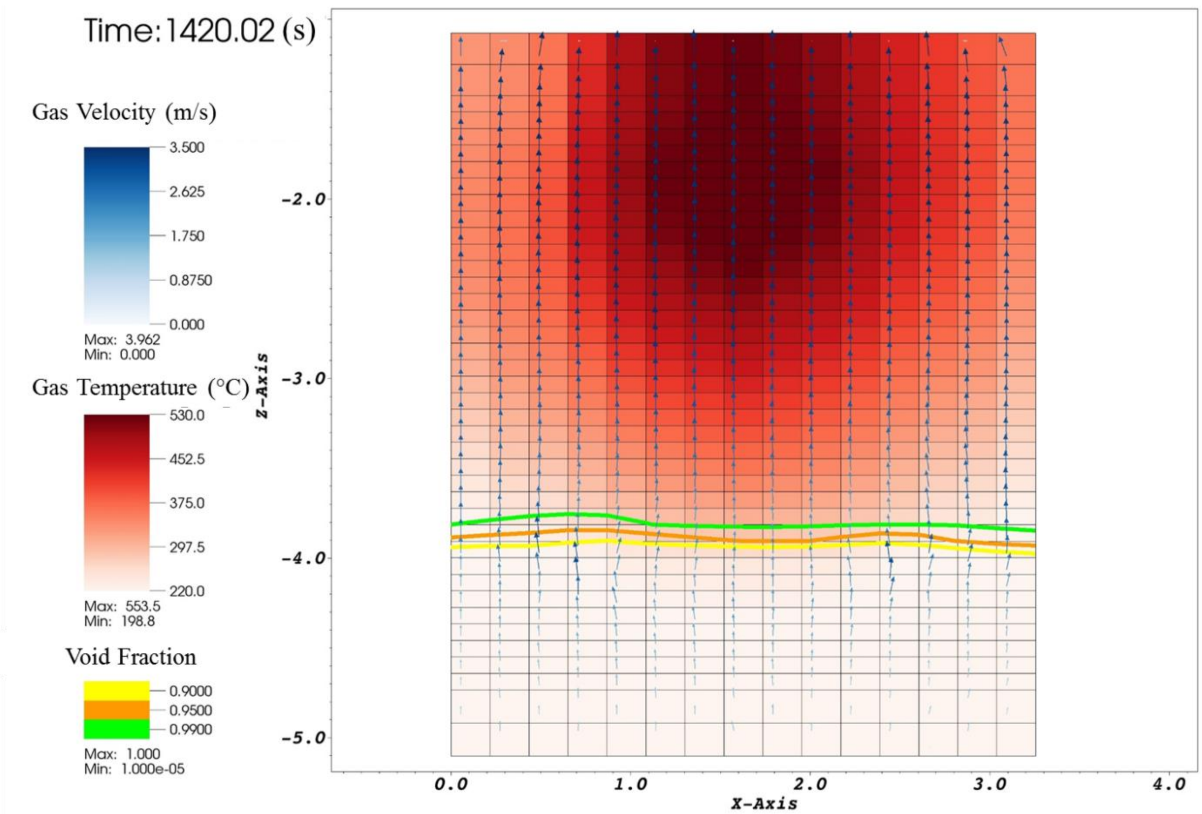

Fig. 10 : Gas velocity, gas temperature fields and void fraction profile during the core reflooding

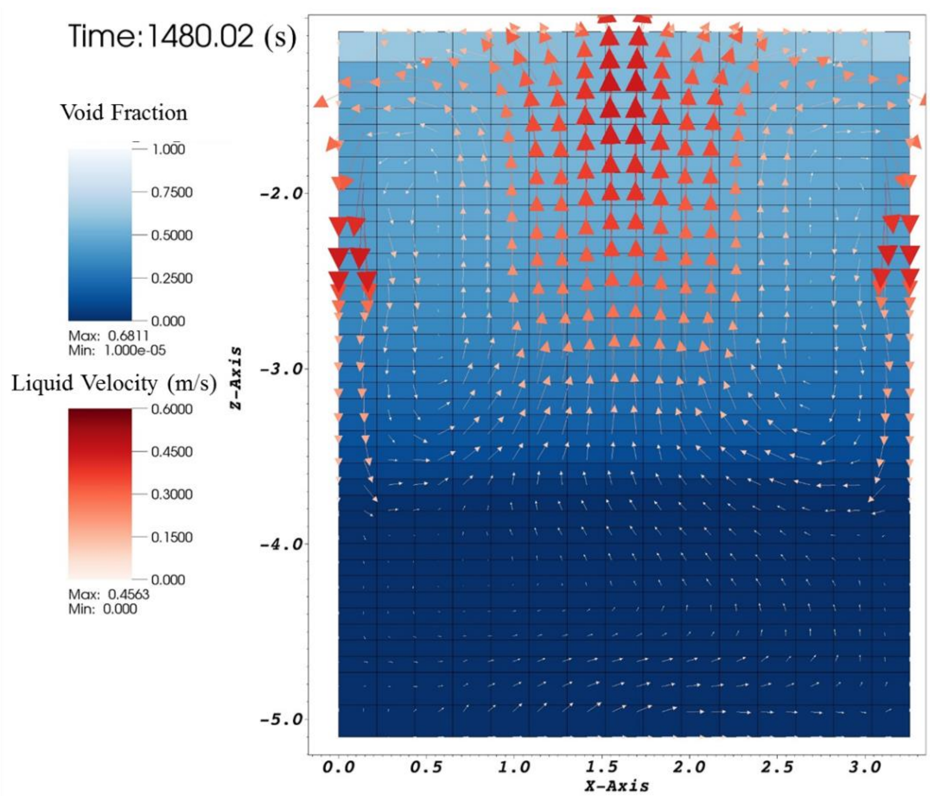

Fig. 11 : Liquid velocity and void fraction fields after the core reflooding